Evaluation of a protective acrylic finish applied to surfaces painted with acrylic paints for outdoor or indoor uses

José S. Pozo-Antonio , Enrique M. Alonso-Villar [*], Teresa Rivas , Iria Márquez

CINTECX, GESSMin Group, Dpto. de Enxeñaría de Recursos Naturais e Medio Ambiente, Universidade de Enxeñaría de Minas e Enerxía, Universidade de Vigo, 36310, Vigo, Spain

A B S T R A C T

Protection of contemporary murals to reduce paint fading caused by exposure to sunlight is currently under study due to a general demand. In this study we evaluated the effectiveness of a commercial protective acrylic finish applied to concrete and brick mock-ups previously painted with different coloured (red and yellow) paints for outdoor and indoor uses. The mock-ups were exposed to an accelerated aging test, with artificial UV irradiation for 3630 h. UV radiation is the most threatening sunlight portion to the paints used in these artworks, inducing mainly fading. Colorimetric measurements were made on the surfaces every 15 days. At the end, aged samples and the respective controls (not subjected to the aging test) were evaluated by stereomicroscopy, X-ray diffraction, Fourier transform infrared spectroscopy and scanning electron microscopy.

Application of the protective finish modified the surface of the paintwork, but generally reduced the rate at which the colour changed. In the mock-ups painted with paint for indoor use without the protective finish, the paintwork degraded faster on brick than on concrete.

The findings highlight the need for appropriate selection of paints depending on where they will be applied and the suitability of using a protective finish depending on the composition of each paint.

1. Introduction

Paint fading, which can be defined as the loss of chroma from the paint film, is one the most common alteration forms in contemporary wall paintings exposed to sunlight [1,2]. Fading affects the paintwork, regardless of the substrate [3].

Although there are no clear guidelines regarding conservation treatments aimed at reducing this type of alteration, international research companies have recently begun to design coatings that can be applied to painted surfaces to provide protection against solar irradiation and thus slow down colorimetric degradation of the paint.

Acrylic paints are most used in murals as they are relatively resistant to environmental conditions. However, acrylic paints are susceptible to photodegradation [4–6]. Therefore, to understand how the paintwork deteriorates, it is important to determine the chemical and physical changes that occur in the paint compounds on exposure to solar radiation. Acrylic paints are composed of an acrylic binder, organic pigments, solvents, extenders, and additives [7–11]. Acrylic binders are based on an emulsion of four basic components: water, monomer, initiator, and surfactant [5]. Pigments are responsible for the colour of the paint.

Solvents allow the paint to flow. Extenders that are poorly soluble in water and preferably inert to acids and alkalis are used to control flow, to improve the strength of the paint film and to modify the gloss of the finish [12]. Rutile (TiO_2) is the most used extender and is also used as opacifier [13]. Moreover, TiO_2 nanoparticles (commonly used as white pigment), which are treated with aluminium and silicon oxyhydrates and zirconium, tin, zinc, cerium and boron oxides and oxhydrates [14], allow absorption of UV radiation and provide photochemical protection of the polymer. Other commonly used extenders include calcite ($CaCO_3$), magnesium carbonate ($MgCO_3$), talc ($Mg_3Si_4O_{10}(OH)_2$) and barite ($BaSO_4$) [12]. The additives used in manufacturing extenders include protective colloids, biocides, freeze-thaw agents, and pH buffers [8,15]. Solar radiation could affect these compounds at different intensities [4–6].

Additives such as those mentioned above are included along with solvents in the paint composition to produce paints that are resistant to environmental agents (light, humidity, and temperature) and are thus suitable for outdoor use. These additions lead to higher concentrations of volatile organic compounds (VOCs) than in paints intended for indoor use. These additions also make outdoor paints more expensive than
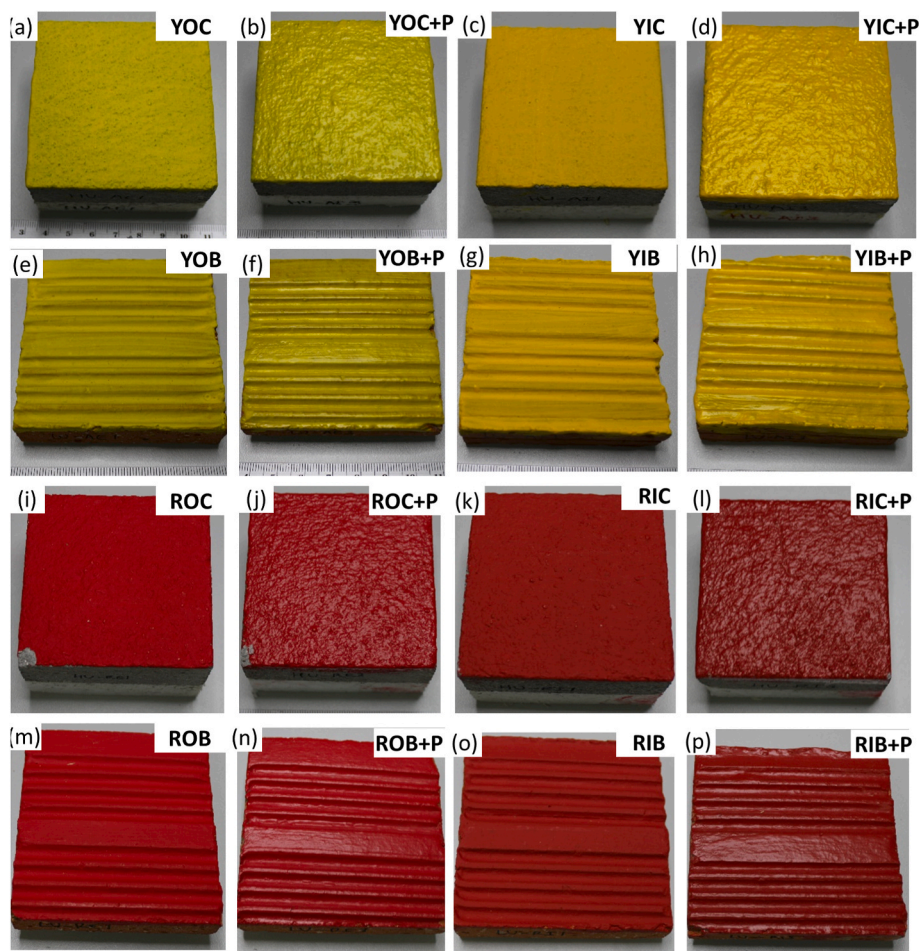

Fig. 1. Digital photographs of the mock-ups (7 × 7x2 cm) used in the study. See Table 1 for explanation of sample identification codes.

paints for indoor uses, and graffiti artists therefore often use or are provided with interior paints to paint outdoor murals.

Regarding the radiation-induced alterations in acrylic polymers, several scientific studies have shown the effects of different types of radiation and different temperatures (UV- radiation for indoor conditions in museums, artificial solar light radiation and dark conditions) on paints and non-pigmented coatings commonly used in the field of cultural heritage conservation, such as water-repellents, consolidants, and anti-graffiti products, mainly applied to glass slide or stone mock-ups [5, 6,16–22]. The ultraviolet portion of solar terrestrial radiation is often considered the most damaging factor causing mainly fading [23]. UV light comprises about 90–95% of UV-A (400–315 nm) and 5–10% of UV-B (315–280 nm), as most of UV-B and UV-C (280–190 nm) is removed by stratospheric ozone. Acrylic polymers are prone to photooxidation via chain scission reactions and cross-linking; chain scissions prevail over cross-linking when the alkyl side groups are shorter [5,18]. For non-pigmented acrylic paints, it has been found that under dark conditions, the acrylic coatings undergo yellowing, a reduction in solubility and an increase in tensile strength attributed to slight cross-linking of the polymer [16]. Exposure to UV radiation induces a slight loss of tensile strength, and the solubility is slightly increased due to breakdown of the polymer by chain-scission reactions [16,17]. In a study with acrylic polymers alone and mixed with inorganic pigments, Pintus et al. [5] observed a decrease in the non-ionic surfactant after UV exposure, which suggests that acrylic binders are sensitive to UV light. These researchers also reported that new products are formed after UV-irradiation, including unspecified aldehydes, lactones and acidic oxidation products.

Considering the effectiveness of polymers in protecting outdoor architectural elements, research has been carried out with stone and concrete substrates [24–29], but the use of polymers to protect paintwork has scarcely been evaluated. A few studies have addressed the use of anti-graffiti products to protect real contemporary wall paintings or painted mock-ups [27,28,30,31]. No previous studies have focused on assessing the effectiveness of protective coatings to reduce the fading due to solar radiation. As these products are mainly composed of acrylic polymers, the deterioration patterns should be similar to those observed in acrylic paints.

As a consequence of the increasing demand for new methods and products to protect public artworks, in 2018, the European Community financed a project entitled Conservation of artworks in Public Spaces (CAPuS), which has defined the methodological bases for the conservation of materials used in urban art, such as contemporary murals [32].

In this research, we evaluated the effectiveness of a protective finish applied to concrete and brick mock-ups previously painted with paints for indoor or outdoor uses. The mock-ups were subjected to an accelerated ageing test with artificial UV irradiation for 3630 h (165 days with 22 h of exposure per day), since the solar terrestrial radiation, ultraviolet portion (90–95% of UV-A and 5–10% of UV-B) is the most aggressive one for paints. Prior to the aging test, the characteristics of the protective coating were determined by stereomicroscopic and spectrophotometric analyses. Spectrophotometric analysis was used to monitor the colorimetric changes on the painted surfaces over time, and aged samples were then evaluated by mineralogical, chemical and physical analyses.

Table 1
Samples used in the research with the corresponding identification (ID) code.

Paint	Intended use	Substrate	Protector	ID
Yellow	Outdoor	Concrete	–	YOC
			Yes	YOC + P
		Brick	–	YOB
			Yes	YOB + P
	Indoor	Concrete	–	YIC
			Yes	YIC + P
		Brick	–	YIB
			Yes	YIB + P
Red	Outdoor	Concrete	–	ROC
			Yes	ROC + P
		Brick	–	ROB
			Yes	ROB + P
	Indoor	Concrete	–	RIC
			Yes	RIC + P
		Brick	–	RIB
			Yes	RIB + P

2. Materials and methods

2.1. Substrates

Two of the most common substrates of contemporary wall paintings in European cities were selected for study: concrete and brick (Fig. 1).

The concrete was prepared using Portland cement CEM II//B-M (V-L) 32.5 N, provided by COSMOS S.A., and commercial siliceous aggregate of grain size 20–50 μm. The concrete formulation was prepared using a weight proportion binder/aggregate ratio of 1/3. Cement and aggregate were mixed manually. Tap water was then added and the paste was stirred manually. The water/binder ratio (w/w) was 0.45. The freshly mixed paste was placed inside a wooden mould (70 × 70 cm) and held under laboratory conditions for 1 month (RH 60 ± 10% and 18 ±5 °C). Mock-ups (16) measuring 7 × 7 × 2 cm were cut from the dried concrete with a diamond cut wheel machine and water.

For the brick samples, simple hollow bricks of 24 × 11 × 4 cm were cut into mock-ups of 7 × 7 × 2 cm with the same cutting machine, to produce a total of 16 samples.

The mock-ups were washed and cleaned with a brush to remove any particles adhered to the surface and then dried in an oven at 40 ± 0.1 °C until constant weight. The mock-ups were stored under laboratory conditions (RH 60 ± 10% and 18±5 °C) for one month before the paints were applied.

2.2. Paints and application

Interior and outdoor paints of different colours (yellow and red), manufactured by PROA [33], were selected for the study. The paints were composed by a water based acrylic dispersion (*P7 Plastica REVE-PROA mate seda*), mixed with the selected pigment. According to the data sheet, this acrylic dispersion is characterized by density of 1.225 ± 0.05 kg L^{-1}, viscosity of 100 ± 10 units (measured in a Krebs viscometer), non-volatile matter content of 55 ± 5% (w/w), liquid water transmission rate of 0.05 kg m^{-2} h^{-1} (following [34]), and water vapour permeability of 0.81 metric perms (following [35]). The use (outdoor or indoor) is given by the pigment mix.

Specifically, for yellow paints:

- Yellow paint for indoor use *P7-amarillo REVEPROA*. According to the supplier's indications, the organic pigment is monoazo yellow. Samples to which this paint were applied were identified by codes beginning with YI (see Table 1).
- Yellow paint for outdoor use *P7-amarillo REVEPROA*. Organic pigment: quinophthalone. Samples were identified by codes beginning with YO (see Table 1).

and for red paints:

- Red paint for indoor use *P7-rojo REVEPROA*. Organic pigment: naphthol. Samples were identified by codes beginning with RI (see Table 1).
- Red paint for outdoor use P7-*rojo REVEPROA*. Organic pigment: perylene red. The samples were identified by codes beginning with RO (see Table 1).

Each paint was applied to four mock-ups (7 × 7 × 2 cm) of each substrate. Following the technical sheets, the paints were applied with a brush, using the required number of brushstrokes to ensure that the supports were completely covered. For the red paints, only one coat was applied while for the yellow paints, three coats were required. The painted mock-ups were dried under laboratory conditions (RH 60 ± 10% and 18±5 °C) for 24 h. After application of the final coat of paint, the samples were held in the laboratory for 7 days to ensure that the paint dried completely.

The letter C for concrete or B for brick were added to the codes used to identify the type of paint (see above) (e.g., YIB refers to yellow paint for indoor use on a brick substrate).

2.3. Protective finish and application

After 7 days, two of the four samples in the same condition (substrate and paint) were coated (with a brush) with the protective finish Proa BV000-*Barniz al agua satinado* (hereinafter + P, see Table 1), again provided by PROA [33]. According to the data sheet, this is a water-based acrylic resin, of density 0.95 ± 0.050 kg L^{-1}, viscosity 110 ± 30 s (in a Ford Viscosity Cup 4 at 20 °C) and a non-volatile matter content of 33 ± 5% (w/w). Only one light coating was applied to each mock-up. The samples were held under laboratory conditions for 1 month.

One of the two samples with the protective coating and one of samples without the coating for each condition (substrate and paint) were exposed to the accelerated aging test using artificial UV light. The other samples were held under laboratory conditions as references for comparative purposes.

Table 1 and Fig. 1 show the samples used in this research.

2.4. Accelerated ageing test by artificial UV irradiation

As was stated in previous researches, UV-A light is the radiation with greatest effect on the fading suffered by paints. Therefore, in the current research the painted surfaces of the sample mock-ups were irradiated using two 300 W OSRAM Ultra Vitalux bulbs with mostly UV-A percentage (13.6 W of UV-A and 1.3 W of UV-B radiation). To achieve a similar maximum irradiation intensity in all cases, the bulbs were placed at 30 cm from each other and at a distance of 50 cm from the surface. The mock-ups were held under the test conditions for a total of 3630 h, corresponding to 165 days with 22 h of exposure per day and 2 h of darkness.

2.5. Analytical techniques

2.5.1. Characterization of the products
To characterize the products, the four paints and the protective finish were each applied to an aluminum support. Scrapings of the dry products were removed and ground to a powder for analysis by Fourier transform infrared spectroscopy (Thermo Nicolet® 6700), in attenuated total reflectance mode (ATR-FTIR) in the middle infrared (IR) spectral region between 400 and 4000 cm^{-1}, with a resolution of 4 cm^{-1} and 20 sample scans.

Moreover, the same powder was examined by X-ray diffraction (SIEMENS D-5000), to characterize the mineralogical composition by the random powder method. Analyses were performed using Cu-Kα
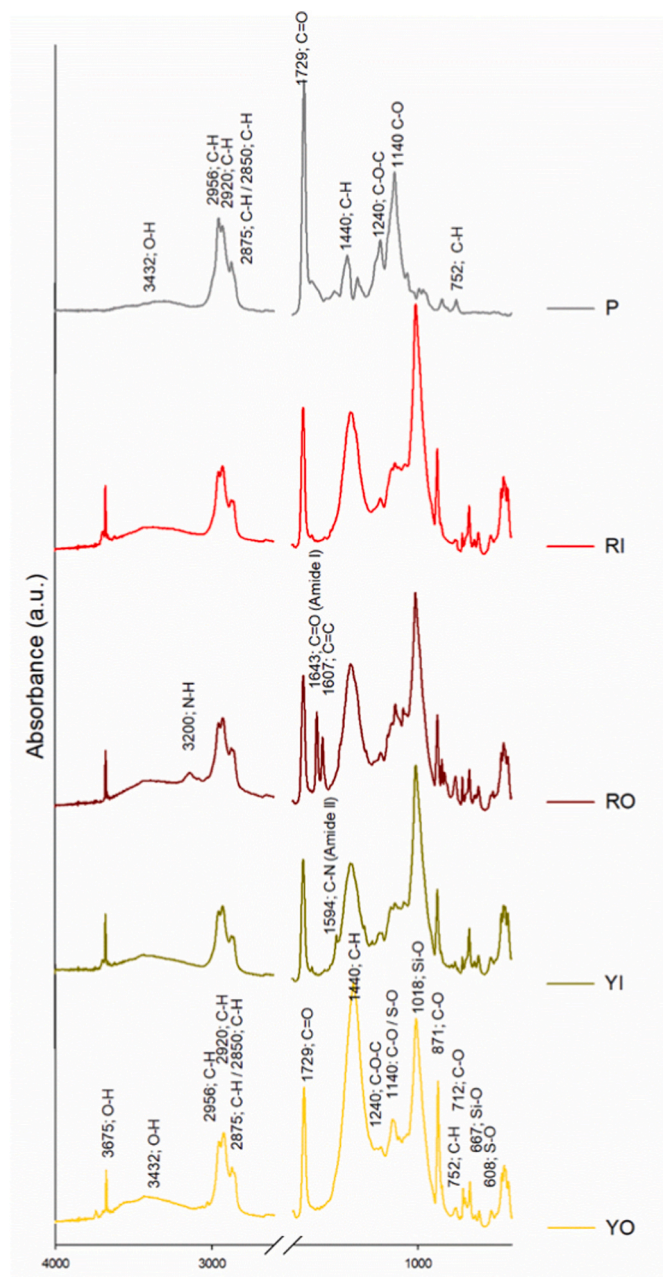
Fig. 2. FTIR (absorbance) spectra of the selected paints and the protective finish. RI: red paint for indoor use. RO: red paint for outdoor use. YI: yellow paint for indoor use. YO: yellow paint for outdoor use. P: protective finish.

radiation, Ni filter, 45 kV voltage, and 40 mA intensity. The exploration range was 3°–60° 2θ and the goniometer speed was 0.05 2θ s^1. Identification of each mineral phase was determined using the X'Pert HighScore.

2.5.2. Evaluation of the appearance of the protective finish on the painted surfaces and of the effectiveness of the coating

To determine the influence of the protective finish on the painted surfaces from an aesthetic point of view, the reference samples (unaged samples) were examined under a stereomicroscope (SMZ800 Nikon).

The colours of the uncoated painted surfaces and of the surfaces coated with the protective finish were characterized using CIELAB and CIELCH colour spaces [36]. In the CIELAB space, *L** (lightness), *a** and *b** (colour coordinates) were measured using a Minolta CM-700d spectrophotometer. *L** is the lightness, which ranges from 0 (absolute black)

Table 2
FTIR fingerprint bands used to identify the nature of the paints and protector and the fillers.

Bond Type	Wavenumber (cm^{-1})	Assigned to:	ID
O–H stretching – intermolecular bonded	3675	Talc	YI, YO, RI, RO
O–H stretching vibration	3200–3550	Acryl	YI, YO, RI, RO, P
C–H stretching	2850–2956	Acryl	YI, YO, RI, RO, P
C=O carbonyl stretching	1729	Acryl	YI, YO, RI, RO, P
C–H bending	1440	Acryl	YI, YO, RI, RO, P
C–O–C asymetric vibration	1240	Acryl	YI, YO, RI, RO, P
C–O stretching	1140	Acrylic	YI, YO, RI, RO, P
S–O stretching	1140	Barite or Barium potassium sulphate	YI, YO, RI, RO
Si–O	1018	Talc	YI, YO, RI, RO
C=O carbonate	871	Calcite	YI, YO, RI, RO
C–H bending	752	Acryl	YI, YO, RI, RO, P
C–O out of plane	712	Calcite	YI, YO, RI, RO
Si–O	667	Talc	YI, YO, RI, RO
S–O bond	608	Barite or Barium potassium sulphate	YI, YO, RI, RO

to 100 (absolute white); *a** indicates the colour position between red (positive values) and green (negative values) and *b** indicates the colour between yellow (positive values) and blue (negative values). In the CIELCH colour space, *L** is the same as described for space CIELAB, the chroma or saturation, *C*$_{ab}$*, corresponds to *C*$_{ab}$* = [(a*)^2 + (b*)^2]$^{1/2}$ and the hue, *h*, is calculated by means of the expression *h* = tan [1 – (a*/b*)]. Twenty measurements were made at random points on each sample to provide statistically consistent results, with each measurement being the average of three. The measurements were made in the Specular Component Included (SCI) mode (the colour evaluation was done considering the total appearance, independent of surface roughness of the bricks and the concrete), for a spot diameter of 3 mm, using D65 as the illuminant and an observer angle of 10°. Colorimetric differences were calculated as colour differences (Δ*L**, Δ*a**, Δ*b**, Δ*C*$_{ab}$* and Δ*H*$_{ab}$*) and total colour change (Δ*E*$_{ab}$*, eq. (1)) relative to the colour of the fresh samples [36].

$$\Delta E^*_{ab} = (\Delta L^{*2} + \Delta a^{*2} + \Delta b^{*2})^{1/2}, \qquad (1)$$

so that higher values indicate more visible colour changes.

To monitor the aging that the samples exposed to the artificial UV radiation underwent, colour measurements were performed every 330 h (15 days), yielding 12 colour measurements for each sample.

At the end of the experiment (3630 h), the surface of samples with Δ*E*$_{ab}$* higher than 3 CIELAB units was scraped, and the powder collected was examined by X-ray diffraction (XRD, random powder method) and ATR-FTIR analyses.

In addition, 1 × 1 cm-scales were removed from the surfaces and their unaged counterparts (for comparative purposes) and after being C-coated they were analysed by scanning electron microscopy with energy-dispersive x-ray spectroscopy (SEM-EDS) (Philips XL30) in both Secondary Electron (SE) and Back Scattered Electron (BSE) modes. Optimum observation conditions were obtained at an accelerating potential of 15–20 kV, a working distance of 9–11 mm and specimen current of 60 mA. The acquisition time for recording EDS spectra, i.e., the dwell time, was 40–60 s.

Table 3

Mineralogical composition revealed by X-ray diffraction analysis (random powder mode) of the paints and protector under study and their concentration (%). n.d.: non-detected. RI: red paint for indoor use. RO: red paint for outdoor use. YI: yellow paint for indoor use. YO: yellow paint for outdoor use. P: protective finish.

Product	Mineralogical composition	Formula	Concentration (%)
RI	Calcite	$CaCO_3$	30-50
	Barite	$BaSO_4$	30-50
	Talc	$Mg_3Si_4O_{10}(OH)_2$	30-50
RO	Calcite	$CaCO_3$	30-50
	Barium Potassium Sulfate	$Ba(K)SO_4$	30-50
	Talc	$Mg_3Si_4O_{10}(OH)_2$	10-30
YI	Calcite	$CaCO_3$	10-30
	Barite	$BaSO_4$	30-50
	Blende	ZnS	10-30
	Talc	$Mg_3Si_4O_{10}(OH)_2$	10-30
	Clinochlore	$Mg_5Al(AlSi_3O_{10})(OH_8)$	3-10
YO	Calcite	$CaCO_3$	30-50
	Barite	$BaSO_4$	30-50
	Talc	$Mg_3Si_4O_{10}(OH)_2$	10-30
	Kaolinite	$Al_2Si_2O_5(OH)_4$	3-10
P	n.d.	n.d.	n.d.

3. Results and discussion

3.1. Paint characterization

The FTIR spectra shown in Fig. 2 enabled the identification of the acrylic nature of these paints and protector; the identification was carried out considering the typical fingerprint bands of each large group of organic polymers (Table 2) [5,6,37]. In all of the paints, the presence of talc ($Mg_3Si_4O_{10}(OH)_2$) and calcite ($CaCO_3$) was detected (Table 2) [40, 41]; this was also confirmed by XRD (Table 3). The XRD analysis also revealed the presence of barite ($BaSO_4$), a white pigment added to paint as and extender [39], in all of the paints except the red paint for outdoor use, which contained barium potassium sulphate ($Ba(K)SO_4$) (Table 3). The presence of molecules with S–O bond was confirmed by FTIR (Table 2) with an absortion peak at 608 cm^{-1}; the peak at 1140 cm^{-1} assigned to C–O stretching can also be attributed to S–O. In addition, XRD analysis (Table 3) revealed the presence of blende (ZnS) and clinochlore ($Mg_5Al(AlSi_3O_{10})(OH)_8$) in the yellow interior paint (YI) and of kaolinite ($Al_2Si_2O_5(OH)_4$) in the yellow paint for outdoor use (YO). Note that although minerals were not detected in all of the paints, they may have been present at concentrations below the detection limit of the equipment (3 wt%)These compounds act as fillers and their use makes it possible to reduce the quantity of solvent, improve paint adhesion and prevent surface defects during curing. Due to their inorganic nature, fillers are not prone to photodegradation. No inorganic compounds were detected in the protective finish (P).

The manufacturer provided information on the nature of the pigments, but without specifying the pigment referred to. However, the FTIR analysis revealed further details (Fig. 2):

- Yellow paint for indoor use (YI): the manufacturer indicated that the pigment was monoazo yellow. This was verified by the presence in the spectrum of bands at 1674 cm^{-1} (C=O absorbance), 1594 cm^{-1} (C–N absorbance), 1517, 1340, 1285 cm^{-1}, which indicate the presence of amides [37,42]; the pigment could be PY3 or PY74 [37].
- Yellow paint for outdoor use (YO): quinophthalone pigment. A band was detected at 1620 cm^{-1}, and the pigment is possibly PY1 [38].
- Red paint for indoor use (RI): naphthol-type pigment. Bands detected at 1674 cm^{-1} (amide I), 1555 cm^{-1} (amide II) and 1324 cm^{-1} could indicate the presence of pigment PR112 [37,42].
- Red paint for outdoor use (RO): perylene-type pigment. The presence of bands at 3200 cm^{-1} (N–H stretching), 1643 cm^{-1} (amide I) and 1607 cm^{-1} (amide I) could indicate the presence of the pigment.
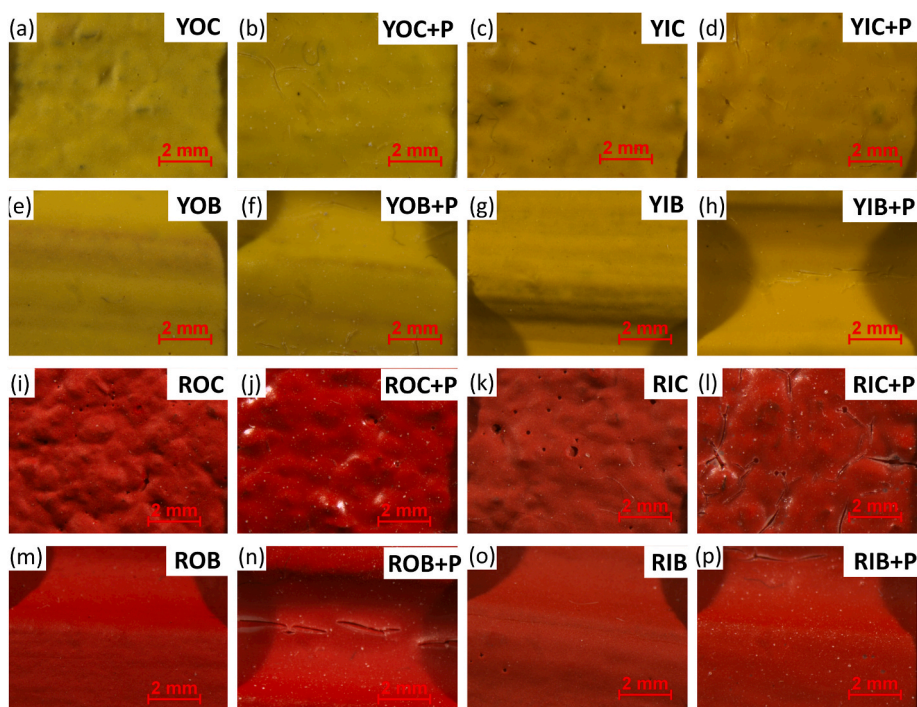

Fig. 3. Stereoscopic micrographs of the surfaces of concrete and brick mock-ups painted with red and yellow paints for indoor or outdoor uses and their counterparts with the protective finish evaluated in this research.
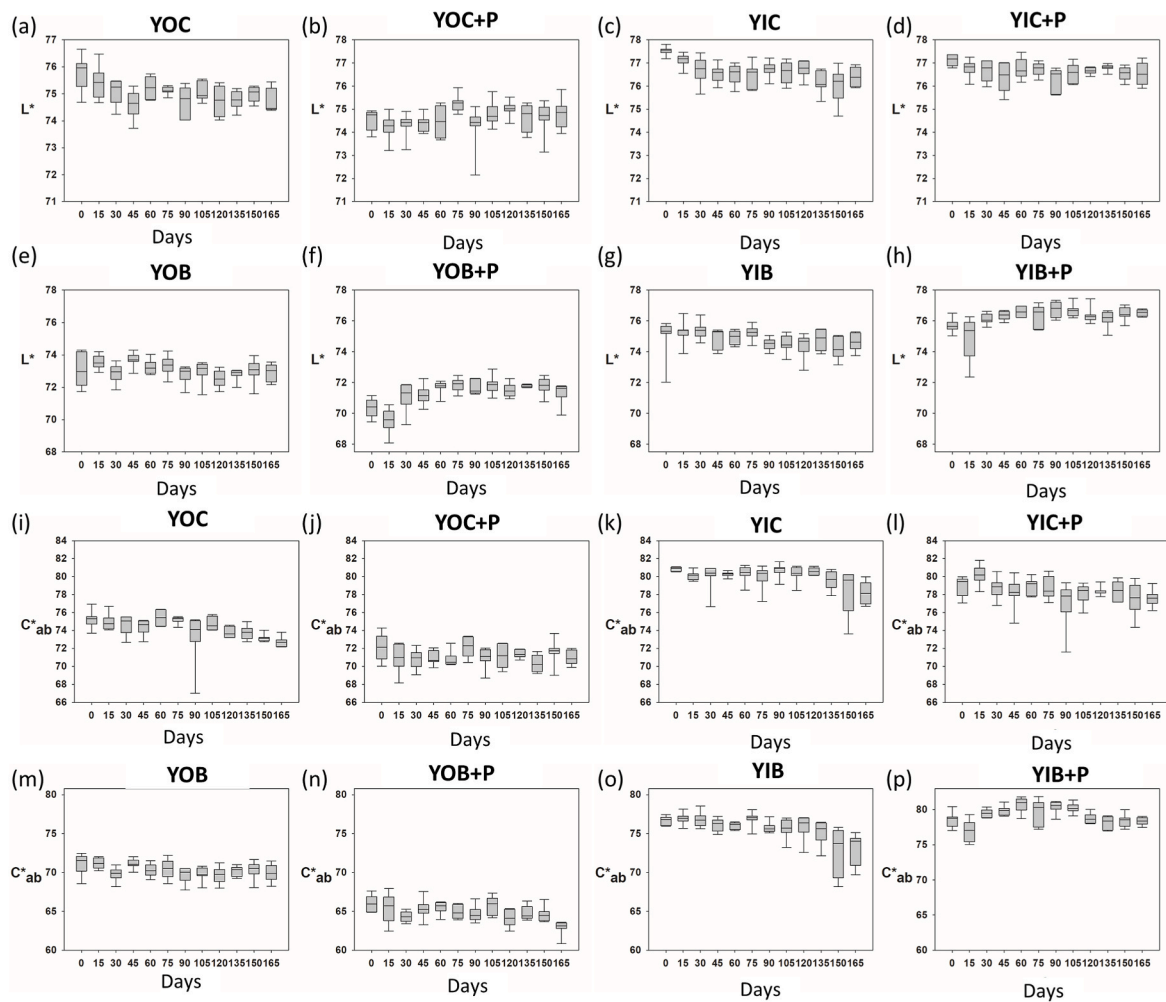
Fig. 4. Box plots of the CIELAB parameters L* (a–h) and C*_{ab} (i–p) for the surfaces of concrete (a-d, i-l) and brick (e-h, m-p) mock-ups painted with yellow paint (without protector-a, c, e, g, i, k, m, o; and with protector-b, d, f, h, j, l, n, p).

Table 4

Colorimetric variations (ΔL^*, Δa^*, Δb^*, ΔC^*_{ab} and ΔH^*) and total colour change (ΔE^*_{ab}) in the protected painted surfaces, considering the surface of the un-protected surfaces as the reference. n = 20.

	ΔL^*	Δa^*	Δb^*	ΔC^*_{ab}	ΔH^*	ΔE^*_{ab}
YIC + P	−0.77	1.04	−0.79	−0.66	−1.12	1.51
YOC + P	−1.55	0.65	−4.33	−4.36	−0.41	4.65
YIB + P	−0.06	1.14	0.20	0.31	−1.11	1.16
YOB + P	−3.54	1.74	−5.62	−5.67	−1.57	6.86
RIC + P	0.69	−2.48	−3.49	−3.95	−1.66	4.34
ROC + P	0.92	−3.63	−4.93	−5.64	−2.39	6.19
RIB + P	0.13	0.09	−0.89	−0.39	−0.80	0.90
ROB + P	0.54	−1.51	−2.69	−2.68	−1.54	3.13

3.2. Effect of the protective coating on the painted surfaces

The micrographs of the painted surfaces before and after application of the protective finish are shown in Fig. 4. For the surface with the protective finish, the protector layer and several fissures were identified, mainly on the surfaces painted with red paints (Fig. 3j, l, n, p). In addition, the glossy appearance caused by the protective coating was more intense on the concrete surfaces painted with red paints (Fig. 3j, l) than in other samples.

Spectrophotometric analysis enabled identification of the aesthetic impact of the protector on the painted surfaces (Table 4). The parameter most affected was b*, with exceptions for the yellow interior paint,

regardless of the substrate (YIC + P, YIB + P), with parameter a* being the most affected in this case. The value of b* decreased, indicating a loss of yellowing coloration. In the samples in which a* was the most affected parameter, the value increased, suggesting a change to a reddish colour. Note that the lightness (L*) decreased (darkening) in the yellow painted surfaces while it increased in the red painted surfaces. Regarding the other parameters, the chroma (C*_{ab}) and the hue (h) decreased in all cases, except for the chroma measured on the YIB + P sample.

Regarding the total colour changes computed and considering that the threshold for a visible colour change by an inexpert observer is 3 CIELAB units [43], only on the samples painted with yellow paint for indoor use, regardless of the substrate (YIC + P, YIB + P), and with red paint for indoor use (RIB + P) yielded $\Delta E^*_{ab}<3$ CIELAB units (indeed, the values were lower than 1.6 CIELAB units). The highest ΔE^*_{ab} corresponded to the samples painted with paints for outdoor uses and with the protective finish, relative to the values registered for the surfaces painted with the interior paints.

It was not possible to identify any influence of the substrate on the ΔE^*_{ab}, as for the concrete sample, the highest ΔE^*_{ab} value corresponded to YOB + P, while in the brick, the highest value corresponded to ROC + P.

3.3. Effectiveness of the protective coating

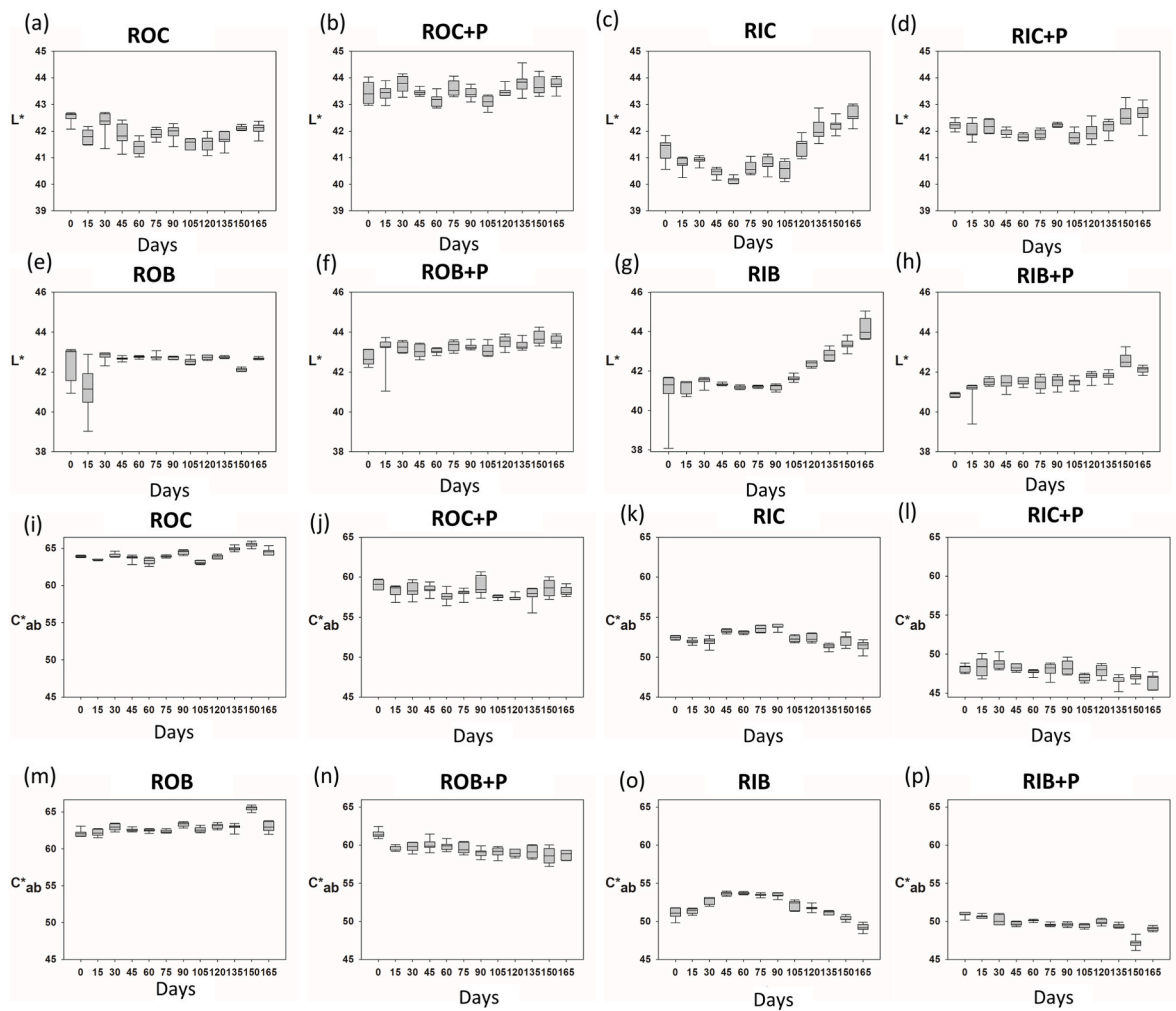Considering the changes in colour over 3630 h (165 days), note that

Fig. 5. Box plots of the CIELAB parameters L* (a–h) and C*ab (i–p) for the surfaces of concrete (a-d, i-l) and brick (e-h, m-p) mock-ups painted with red paint (without protector a, c, e, g, i, k, m, o; with protector b, d, f, h, j, l, n, p).
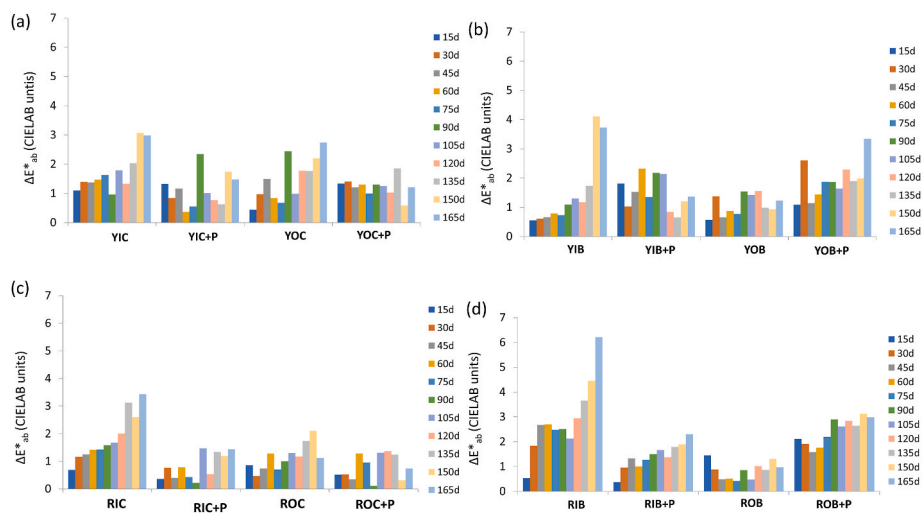

Fig. 6. Changes in ΔE*ab (CIELAB units) throughout 165 days on the surfaces of concrete (a,c) and brick (b,d) mock-ups painted with yellow (a, b) and red (c, d) paints (with and without the protective finish).

L* and C*ab did not undergo intense modifications (yellow painted surfaces: Fig. 4; red painted surfaces: Fig. 5). For the unprotected surfaces, the greatest variations were detected in the samples painted with

paints for indoor use, especially red, i.e., with L* for RIC (Fig. 5c) and RIB (Fig. 5g) and with the C*ab for YIB (Fig. 4o) and RIB (Fig. 5o).

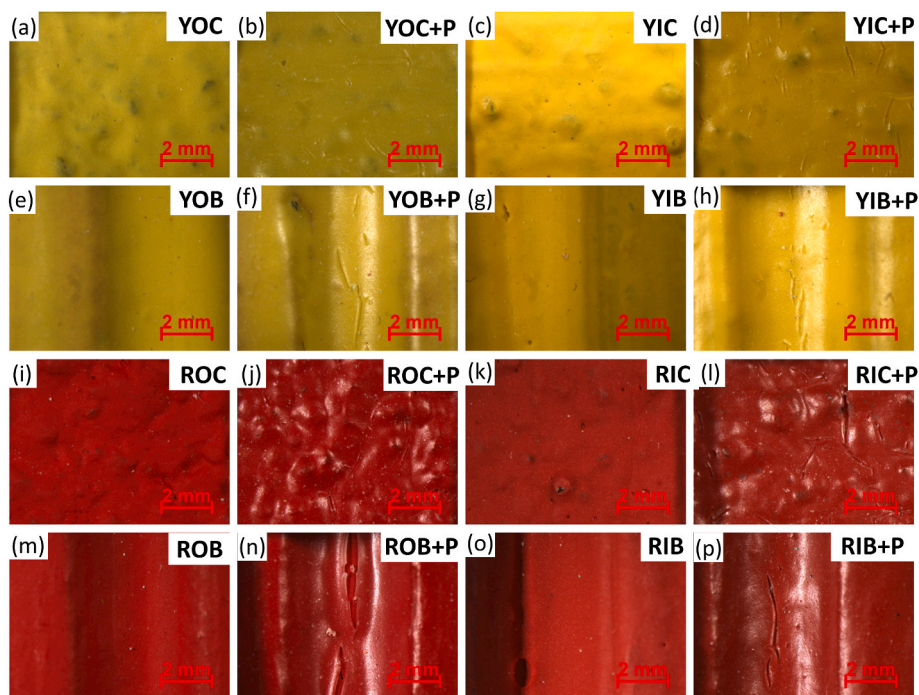Regarding the surfaces coated with the protective finish, the

Fig. 7. Stereomicrographs of the surfaces of concrete and brick mock-ups painted with red and yellow paints for indoor or outdoor uses with and without the protective finish evaluated in this research, after being exposed during 3630 h in an accelerated aging test with artificial UV irradiation.

lightness (L*) generally increased over time (yellow painted surfaces: Fig. 4b,d,f,h; red painted surfaces: Fig. 5b,d,f,h), although the differences among the measurements over time were not statistically significant. The increases were more intense in the painted concrete mock-ups. However, some of the L* values in brick mock-ups showed statistically significant differences over time, such as YOB + P for the L* measured from day 75 to day 150 (Fig. 4f) and RIB + P for the L* measured from day 30 until the end of the test (Fig. 5h).

Regarding the total colour change (ΔE^*_{ab}, Fig. 6) during the aging test, unprotected samples showed increases in ΔE^*_{ab} over time, mainly for the interior paints on the brick mock-ups (YIB and RIB, Fig. 6b and d respectively). This finding suggests the high susceptibility of interior paints to fading, particularly when the paint is applied to brick.

Comparing ΔE^*_{ab} of the protected samples with those of the respective samples without the protective finish.

I) For the concrete samples (Fig. 6a,c), the ΔE^*_{ab} decreased, suggesting effective performance of the protective finish.
II) For the brick samples (Fig. 6b,d), the ΔE^*_{ab} decreased for the paints for indoor use -YIB + P (Fig. 6b) and RIB + P (Fig. 6d)- while it increased for the paints for outdoor use -YOP + B (Fig. 6b) and ROB + P (Fig. 6d). This finding appears to indicate that the protective finish covering paints for outdoor use applied to brick did not satisfactorily conserve the colour of the paint (regardless of the composition).

At the end of the experiment (165 days), the sample with the highest ΔE^*_{ab} was RIB (ΔE^*_{ab}: 6.21 CIELAB units, Fig. 6d), followed by YIB (ΔE^*_{ab}: 3.73 CIELAB units, Fig. 6b), RIC (ΔE^*_{ab}: 3.44 CIELAB units, Fig. 6c) and YOB + P (ΔE^*_{ab}: 3.34 CIELAB units, Fig. 6b); the ΔE^*_{ab} was lower than 3 CIELAB units for the other samples. Therefore, the samples with ΔE^*_{ab} higher than 3 CIELAB units and the respective control samples (not artificially aged) were examined by XRD, FTIR and SEM-EDS to help determine the reasons for these colour changes.

Micrographs of the samples after exposure to the artificial aging test are shown in Fig. 7. No remarkable changes were observed relative to the samples before the test (Fig. 3). After the aging test, samples YIC + P,

Table 5
Mineralogical composition of the aged samples showing a ΔE^*_{ab} higher than 3 CIELAB units. The mineralogical compositions of the samples not subjected to the aging test are also showed.

Samples	Condition	Mineralogical phase
RIB	Before aging test	Calcite, $CaCO_3$
		Talc, $Mg_3Si_4O_{10}(OH)_2$
		Barite, $BaSO_4$
	After aging test	Calcite, $CaCO_3$
		Talc, $Mg_3Si_4O_{10}(OH)_2$
		Silica, SiO_2
		Barite, $BaSO_4$
YIB	Before aging test	Calcite, $CaCO_3$
		Talc, $Mg_3Si_4O_{10}(OH)_2$
		Barite, $BaSO_4$
		Quartz, SiO_2
		Microcline, $KAlSi_3O_8$
	After aging test	Calcite, $CaCO_3$
		Barite, $BaSO_4$
		Talc, $Mg_3Si_4O_{10}(OH)_2$
RIC	Before aging test	Calcite, $CaCO_3$
		Quartz, SiO_2
		Talc, $Mg_3Si_4O_{10}(OH)_2$
	After aging test	Calcite, $CaCO_3$
		Quartz, SiO_2
		Talc, $Mg_3Si_4O_{10}(OH)_2$
		Barite, $BaSO_4$
		Clinochlore,
YOB + P	Before aging test	Calcite, $CaCO_3$
		Barite, $BaSO_4$
		Talc, $Mg_3Si_4O_{10}(OH)_2$
	After aging test	Calcite, $CaCO_3$
		Quartz, SiO_2
		Talc, $Mg_3Si_4O_{10}(OH)_2$
		Illite, $(K,H_3O)(Al,Mg,Fe)_2(Si,Al)_4O_{10}[(OH)_2,(H_2O)]$
		Barite, $BaSO_4$

YOB + P and ROC + P (Fig. 7d, f and 7j respectively) displayed more fissures than before the test (Fig. 3d, f and 3j respectively). After the aging test, sample RIC (Fig. 7k) showed dark spots at some points which
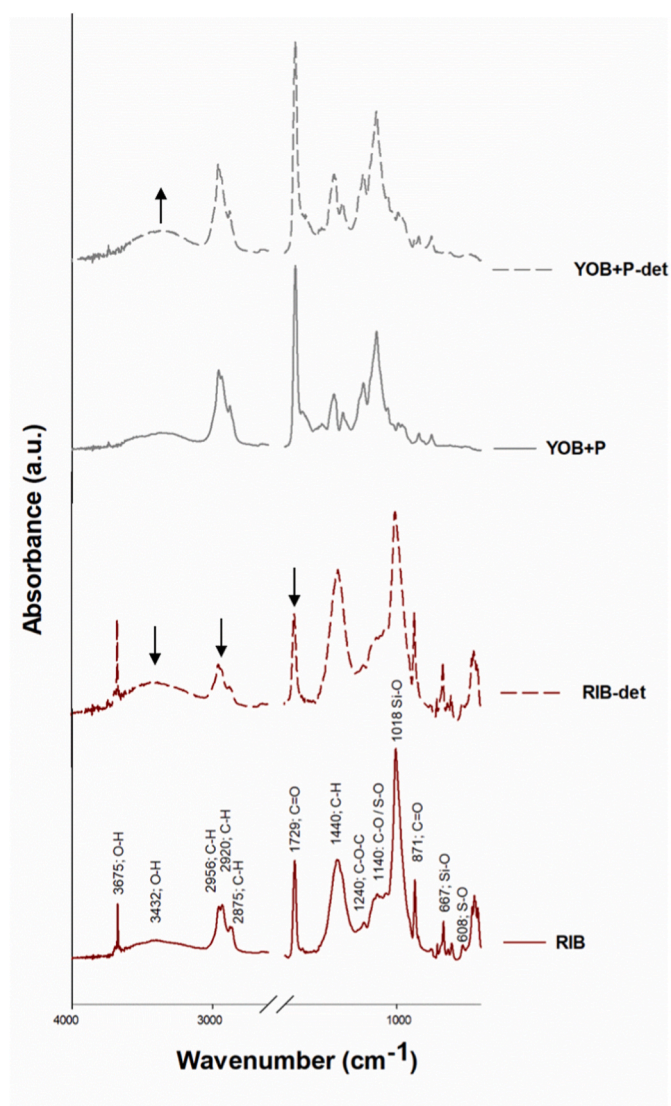
Fig. 8. FTIR (absorbance) spectra of the artificially aged and unaged (-det) RIB and YOB + P mockups.

were not observed before the aging test (Fig. 3k).

Regarding the mineralogical composition of the samples in which colour changes (ΔE^*_{ab}) were more than 3 CIELAB units (Table 5), after the aging test, neoformed minerals were not identified in the material scraped from the surfaces. In addition to the minerals identified as extenders in the paints, mineral phases from the substrates (i.e., quartz, microcline, illite, etc.) were found to have been extracted from the surface during the scraping.

The aged samples for which ΔE^*_{ab} was higher than 3 CIELAB units (RIB, YIB, RIC and YOB + P) and the unaged counterparts were analysed by FTIR. The most representative FTIR spectra are included in Fig. 8.

Taking the O–H intermolecular bonded band at 3675 cm^{-1} (corresponding to the talc) as reference, the RIB (Fig. 8) and YIB paints underwent the greatest changes in the test; the bands that decreased most in intensity were those corresponding to C=O carbonyl stretching (1729 cm^{-1}) and C–H stretching (2956-2850 cm^{-1}). The reduction in the intensity of the band corresponding to C=O was attributed to partial loss of carbonyl groups [18,19,44] whereas reduction in the intensity of the band corresponding to C–H stretching may be associated with hydrogen abstraction processes related to destruction of the polymer backbone structure [18,19]. The bands corresponding to C–H bending (1440 cm^{-1}) and C–O–C bonds (1240 cm^{-1}). also decreased (to a lesser

extent). In sample RIC, the intensity of these bands decreased, whereas in YOB + P the band intensity scarcely decreased (Fig. 8). In these samples (RIC and YOB + P) an increase in the intensity of the band corresponding to O–H stretching (3550-3200 cm^{-1}) was detected (Fig. 8); this increase may be due to oxidation processes [45]. Regarding the pigments, no relevant changes were found comparing the spectra.

SEM analysis provided an exhaustive characterization of the texture of samples with ΔE^*_{ab} higher than 3 CIELAB units. For the sample with the highest ΔE^*_{ab} (RIB, ΔE^*_{ab}: 6.21 CIELAB units) SEM micrographs and EDS spectra (Fig. 9) enabled us to characterize the composition and the texture of the unaged and aged (Fig. 9a–c and d-f, respectively) samples. The acrylic paint is composed by a mixture of granular particles embedded in a C-rich matrix. The main components of the paint were Si, Ca, Mg, S, Ba, Na, Al and Cl (Fig. 9a EDS 1). These elements were derived from the different minerals detected by XRD: calcite (CaCO$_3$), talc (Mg$_3$Si$_4$O$_{10}$(OH)$_2$) and barite (BaSO$_4$). Cl may originate from the organic pigment used in this paint, probably PR112. Although the EDS spectra showed the general composition of the surrounding the point measured, calcite grains could be identified by the presence of Ca (Fig. 9b EDS 2), barite grains were identified as being rich in S and Ba (Fig. 9b EDS3) and blende grains rich in S and Zn (Fig. 9b EDS4). Although blende was not identified by XRD in the red interior paint (RI), this can be explained due to the concentration being lower than the detection limit of the equipment (3 wt%).

After the aging by artificial sunlight, sample RIB also showed accumulation of different mineral grains (mixture of calcite, barite, talc-Fig. 9d EDS6; barite- Fig. 9e EDS7; talc- Fig. 9e EDS8). Therefore, no mineralogical changes were identified in the RIB sample after aging as shown by XRD. Conversely to the unaged RIB, C-rich deposits were identified on the surface of the samples (Fig. 9d EDS 5).

Use of SE mode (Fig. 9c, f) enabled us to detect changes in the texture of the paint after the aging test. The surface of the aged samples was more irregular and loss of the organic layer that binds the grains was evident (Fig. 9f).

The sample with the second highest ΔE^*_{ab} (3.73 CIELAB units), i.e. YIB (Fig. 10a–f), also showed an agglomeration of micrometric grains of different minerals. The general EDS spectrum of this yellow paint for indoor use showed the presence of Si, Mg, Ca, Al, S, Ba, Na and P (Fig. 10a EDS1). Among the minerals identified, calcite (Fig. 10b EDS2), talc (Fig. 10b EDS3) and barite (Fig. 10b, EDS4) were associated with the EDS obtained. After the aging test, the same minerals were identified by SEM (Fig. 10e, EDS5-7). As reported for the RIB sample, the surface of the aged sample was more irregular surface than that of the sample before aging (Fig. 10f, c respectively).

After the aging test, in sample YOB + P (Fig. 10g–j), with a ΔE^*_{ab} of 3.34 CIELAB, the protective finish had more fissures (Fig. 10i) than the samples not subjected to the aging test (Fig. 10g). In this sample, the paint layer was visible through the protector layer. Moreover, at higher magnification, we observed that the surface of the protective finish was more irregular (Fig. 10j) on the aged surface than that on the unaged surface (Fig. 10h).

Sample RIC (Fig. 11a–f) with a ΔE^*_{ab}: 3.44 CIELAB units, did not show any changes in the composition after the artificial aging (Fig. 11a, b, d and e and their respective EDS spectra); however, the surface texture was very different, as the surface of the artificially deteriorated paint (Fig. 11f) was less compact and more irregular than that of the unaged sample (Fig. 11c).

For protected painted surfaces in which the ΔE^*_{ab} was very low, such as sample ROC + P (Fig. 11g–i), (ΔE^*_{ab} of 0.74 CIELAB units), in contrast to the findings for YOB + P, the texture did not change during the aging test (Fig. 11h,f).

4. Conclusions

The effectiveness of an acrylic protective finish on coats of red and yellow paints intended for indoor and outdoor uses was evaluated by
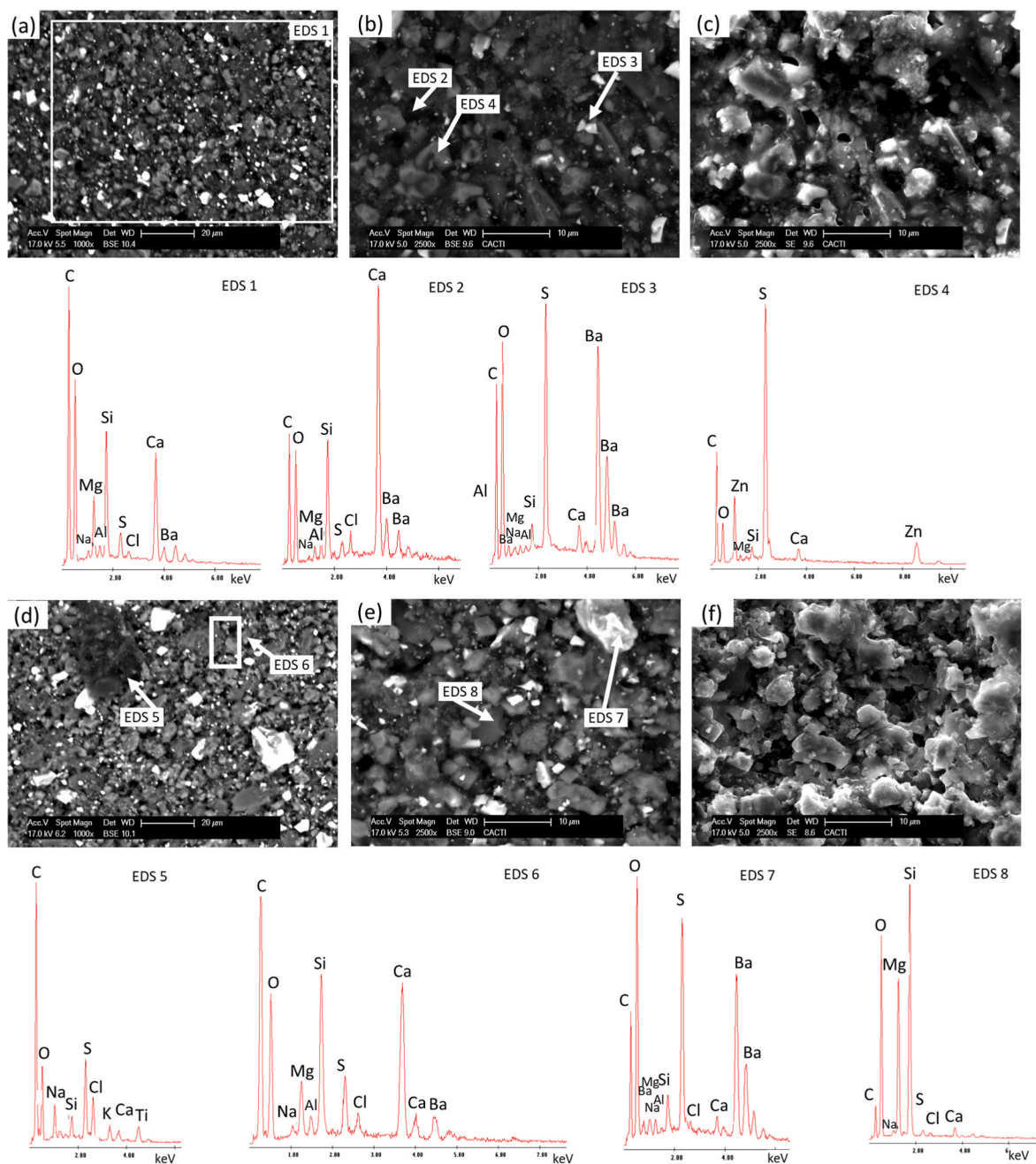
Fig. 9. Stereomicrographs of the control (not aged) RIB sample (a–c) and the artificially aged samples (d–f). EDS spectra are also shown.

exposing concrete and brick mock-ups to an accelerated aging test by artificial UV irradiation for 3630 h (165 days).

Considering the paintwork without the protective finish, the interior formulations degraded more than the formulations for outdoor use. In addition, the interior paints applied to brick degraded more than those applied to concrete, while the opposite occurred with the paints for outdoor use, which degraded more rapidly on concrete than on brick.

Application of the protective finish slowed down the colour change in all the paints, except the outdoor paints applied to brick. Application of the protector modified the appearance of the painted surfaces, giving them a glossy finish. In addition, once the coating was dry, fissures appeared to the depth of the painted surface, making it susceptible to the action of weathering agents. The paints that underwent the greatest colour changes after application of the protective coating were the yellow paint for outdoor use (independently of the type of surface) and the red paints applied to concrete (independently of whether it was

interior or outdoor paint). FTIR confirmed chemical changes (hydrogen abstraction processes related to destruction of the polymer backbone structure and oxidation processes) in the binder of the paints, while the pigments seem to behave stable, since changes of their absorption bands were not detected.

Therefore, the outdoor paints were found to be more suitable than interior paints for creating contemporary murals (street art). Application of a protective coating may slow down the colour changes in this type of paintwork, although the type of paint and the surface on which the murals are painted must be considered, as the colour changes brought caused by the protective coating may affect the artistic integrity of the work.

CRediT authorship contribution statement

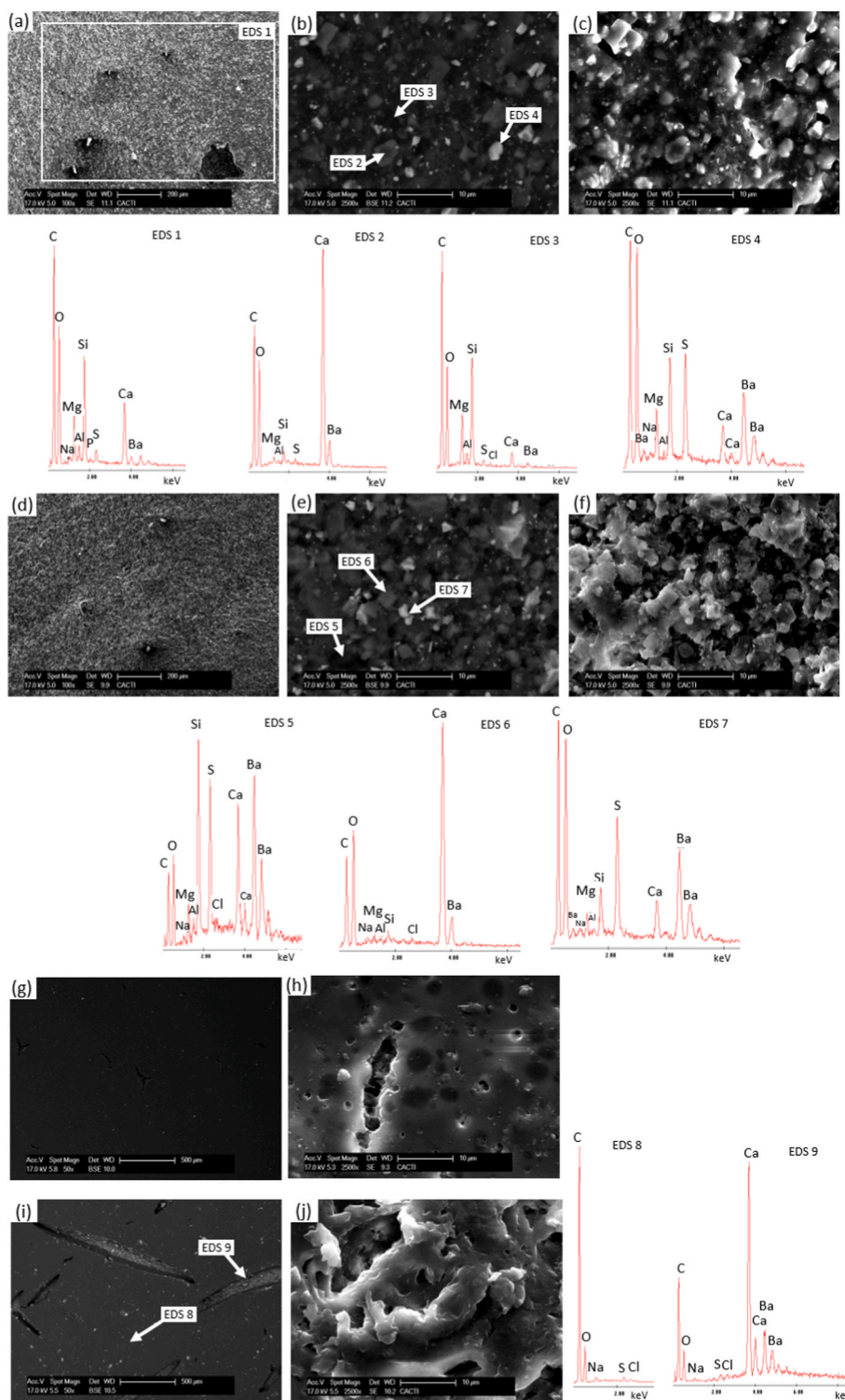**José S. Pozo-Antonio:** Conceptualization, Investigation, Resources,

Fig. 10. Stereomicrographs of the control (not aged) YIB sample (a–c) and the artificially aged sample (d–f) and of the control YOB + P sample (g–h) and the aged sample (g–j). EDS spectra are also shown.

Methodology, Software, Data curation, Visualization, Supervision, Project administration, Writing – original draft, preparation, Writing – review & editing, and, Funding acquisition. **Enrique M. Alonso-Villar:** Investigation, Methodology, Software, Data curation, and, Writing – original draft, preparation. **Teresa Rivas:** Conceptualization, Resources, Methodology, Supervision, and, Funding acquisition. **Iria Márquez:** Investigation, Methodology, Software, and, Data curation.

Declaration of competing interest

The authors declare that they have no known competing financial interests or personal relationships that could have appeared to influence the work reported in this paper.
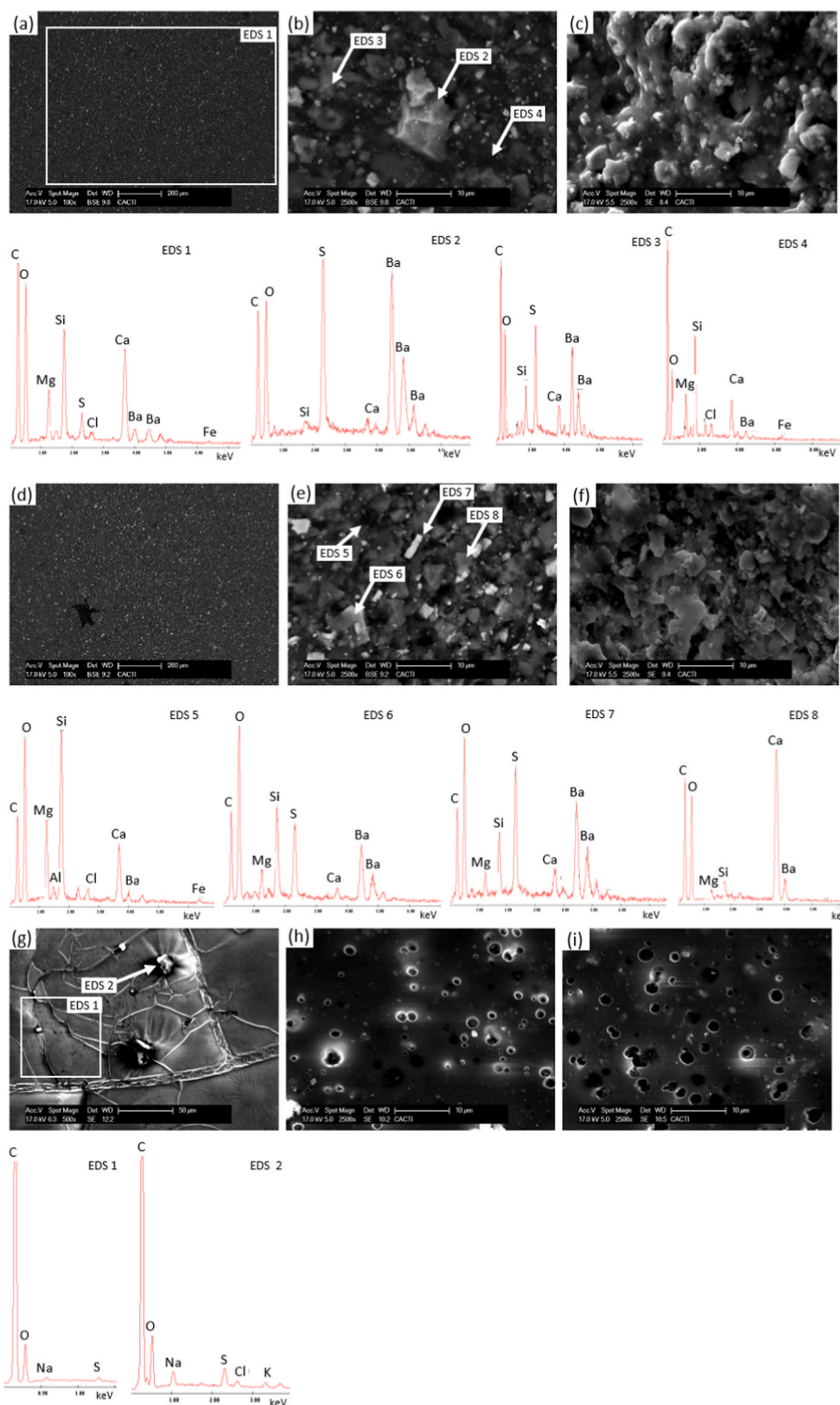
Fig. 11. Stereomicrographs of the control (not aged) RIC sample (a–c) and of the aged sample (d–f) and of the control ROC + P sample (g–h) and the aged sample (i). EDS spectra are also depicted.

References

[1] EwaGlos. In: Weyer A, Roig P, Pop D, Cassar J, Özköse A, Vallet JM, Srsa I, editors. European Illustrated Glossary of Conservation terms for wall paintings and architectural surfaces. Germany: Petersberg; 2015, ISBN 978-3-7319-0260-7.

[2] Glossary – CAPuS. 2021. https://capusproject.eu/glossary/. [Accessed 19 March 2022].

[3] Alonso-Villar EM, Rivas T, Pozo-Antonio JS. Resistance to artificial daylight of paints used in urban artworks. Influence of paint composition and substrate. Prog Org Coating 2021;154:106180. https://doi.org/10.1016/j.porgcoat.2021.106180.

[4] Shultz AR. Degradation of polymethyl methacrylate by ultraviolet light. J Phys Chem 1961;65:967–72. https://doi.org/10.1021/j100824a019.

[5] Pintus V, Wei S, Schreiner M. Accelerated UV ageing studies of acrylic, alkyd, and polyvinyl acetate paints: influence of inorganic pigments. Microchem J 2016;124: 949–61. https://doi.org/10.1016/j.microc.2015.07.009.

[6] Cogulet A, Balnchet P, Labdry V. Evaluation of the impacts of four weathering methods on two acrylic paints: showcasing distinctions and particularities. Coatings 2019;9:121. https://doi.org/10.3390/coatings9020121.

[7] Christie RM. Colour chemistry. The Royal Society of Chemistry; 2001. https://doi.org/10.1039/9781847550590.

[8] Bieleman J. Additives for coatings. Weinheim (Federal Republic of Germany): WILEY-VCH Verlag GmbH; 2000. https://doi.org/10.1002/9783527613304. D-69469.

[9] Bamfield P. Chromic phenomena the technological applications of colour chemistry. The Royal Society of Chemistry; 2001. https://doi.org/10.1039/9781849731034.

[10] Weldon DG. Failure Analysis of paints and coatings. John Wiley & Sons, Ltd; 2009, ISBN 978-0-470-69753-5. p. 372. https://doi.org/10.1002/9780470744673.

[11] Sanmartin P, Capitelli F, Mitchell R. Current methods of graffiti removal: a review. Construct Build Mater 2014;71:363–74. https://doi.org/10.1016/j.conbuildmat.2014.08.093.

[12] Marrion A. The chemistry and physics of coatings. The Royal Society of Chemistry; 2014, ISBN 0-85404-656-9. https://doi.org/10.1039/9781847558206.

[13] Abel A. Pigments for paints. In: Lambourne R, Strivens TA, editors. Paints in surface coatings: theory and practice. Cambridge: Woodhead Publishing; 1999.

[14] Allen NS, McIntyre RB, Maltby J, Hill C, Edge M. Photo-stabilisation and UV blocking efficacy of coated macro and nano-rutile titanium dioxide particles in paints and coatings. J Polym Environ 2018;26:4243–57. https://doi.org/10.1007/s10924-018-1298-0.

[15] Learner T. The analysis of synthetic paints by pyrolysis-gas chromatography-mass spectrometry (PyGCMS). Stud Conserv 2001;46. https://doi.org/10.2307/1506773.

[16] Whitmore PM, Colaluca VG. The natural and accelerated aging of an acrylic artist's medium. Stud Conserv 1995;40(1):51–64. https://doi.org/10.2307/1506611.

[17] Melo MJ, Bracci S, Camaiti M, Chiantore O, Piancenti F. Photodegradation of acrylic resins used in the conservation of stone. Polym Degrad Stabil 1999;66. https://doi.org/10.1016/S0141-3910(99)00048-8. 23-3.

[18] Chiantore O, Trossarelli L, Lazzari M. Photooxidative degradation of acrylic and methacrylic polymers. Polymer 2000;41:1657–68. https://doi.org/10.1016/S0032-3861(99)00349-3.

[19] Chiantore O, Lazzari M. Photo-oxidative stability of Paraloid acrylic protective polymers. Polymer 2001;42:17–27. https://doi.org/10.1016/S0032-3861(00)00327-X.

[20] Learner T, Chiantore O, Scalarone D. Ageing studies of acrylic emulsion paints. In: Vontobel R, editor. 13th triennial metting, rio de Janeiro, 22-27 September 2002, prepints, ICOM committee for conservation. London: James & James; 2002. p. 911–9.

[21] Scalarone D, Chiantore O, Learner T. Ageing studies of acrylic emulsion paint, part II: comparing formulations with poly (EA-co-MMA) and poly (n-BA-co-MMA) binders. In: Verger I, editor. 14th triennial meeting the Hague, 12-16 September 2005, prepints, ICOM committee for conservation, vol. 1. London: James & James; 2005. p. 350–7.

[22] Doménech-Carbó MT, Silva MF, Aura-Castro E, Fuster-López L, Kröner S, Martínez-Bazán ML, et al. Study of behavior on simulated daylight ageing of artists' acrylic and poly(vinyl acetate) paint films. Anal Bioanal Chem 2011;399(9):2921. https://doi.org/10.1007/s00216-010-4294-3.

[23] Jost C, Muehlethaler C, Massonnet G. Forensic aspects of the weathering and ageing of spray paints. Forensic Sci Int 2016;258:32–40. https://doi.org/10.1016/j.forsciint.2015.11.001.

[24] Alessandrini G, Aglietto M, Castelvetro V, Ciardelli F, Peruzzi R, Toniolo L. Comparative evaluation of fluorinated and un fluorinated acrylic copolymers as water-repellent coating materials for stone. J Appl Polym Sci 2000;76:962–77. https://doi.org/10.1002/(SICI)1097-4628(20000509)76:6<962::AID-APP24>3.0.CO;2-Z.

[25] Manodis PN, Tsakalof A, Karapanagiotis I, Zuburtikudis I, Panayiotou C. Fabrication of superhydrophobic surfaces for enhanced stone protection. Surf Coat Technol 2009;703:1322–8. https://doi.org/10.1016/j.surfcoat.2008.10.041.

[26] De Rosario I, Elhaddad F, Pan A, Benavides R, Rivas T, Mosquera MJ. Effectiveness of a novel consolidant on granite: laboratory and in situ results. Construct Build Mater 2015;76:140–9. https://doi.org/10.1016/j.conbuildmat.2014.11.055.

[27] Carmona-Quiroga PM, Jacobs RMJ, Martínez-Ramírez S, Viles HA. Durability of anti-graffiti coatings on stone: natural vs accelerated weathering. PLoS One 2017; 12(2):e017234. https://doi.org/10.1371/journal.pone.0172347.

[28] Carmona-Quiroga PM, Jacobs RMJ, Viles HA. Weathering of two anti-graffiti protective coatings on concrete paving slabs. Coatings 2017;7(1):1. https://doi.org/10.3390/coatings7010001.

[29] Pozo-Antonio JS, Otero J, Alonso P, Mas i Barberà X. Nanolime- and nanosilica-based consolidants applied on heated granite and limestone: effectiveness and durability. Construct Build Mater 2019;201:852–70. https://doi.org/10.1016/j.conbuildmat.2018.12.213.

[30] Pozo-Antonio JS, Jacobs RMJ, Viles HA, Rivas T, Carmona-Quiroga PM. Effectiveness of commercial anti-graffiti treatments in two granites of different texture and mineralogy. Prog Org Coating 2018;116:70–82. https://doi.org/10.1016/j.porgcoat.2017.12.014.

[31] Macchia A, Ruffolo SA, Rivaroli L, Malagodi M, Licchelli M, Rovella N, et al. Comparative study of protective coatings for the conservation of Urban Art. J Cult Herit 2020;41:232–7. https://doi.org/10.1016/j.culher.2019.05.001.

[32] CAPuS- conservation of artworks in public spaces. www.capusproject.eu.

[33] Pinturas PROA website. https://pinturasproa.com. [Accessed 19 March 2022].

[34] UNE-EN 1602. Thermal insulating products for building applications - determination of the apparent density. 2013. 2013.

[35] UNE-EN ISO 7783-2. Paints and varnishes - coating materials and coating systems for exterior masonry and concrete - part 2: determination and classification of water-vapour transmission rate (permeability). 1999. 1999.

[36] CIE S014-4/E. Colorimetry Part 4: CIE 1976 L*a*b* colour space. Vienna: Commission Internationale de l'eclairage; 2007. CIE Central Bureau, 2007.

[37] Learner T. Analysis of modern paints. GCI Publications; 2005, ISBN 0892367792.

[38] Derrick MR, Stulik D, Landry JM. Infrared Spectroscopy in conservation science. Los Angeles: The Getty Conservation Institute; 2009.

[39] Buxbaum G, Pfaff G. Industrial inorganic pigments. Weinheim, Germany: WILEY-VCH Verlag GmbH & Co KGaA; 2005. https://doi.org/10.1002/3527603735.

[40] Castillo LA, Barbosa SE, Maiza P, Capiati NJ. Surface modifications of talcs. Effects of inorganic and organic acid treatments. J Mater Sci 2011;46:2578–86.

[41] Pathak RP, Pankaj S, Ratnam M. Characterisation of leachate material from dam concrete by X-ray diffractometer and FTIR. Int J Res Chem Environ 2012;2(4):58–63.

[42] Lomax SQ, Learner T. A review of the classes, structures, and methods of analysis of synthetic organic pigments. J Am Inst Conserv 2006;45(2):107–25.

[43] Witzel RF, Burnham RW, Onley JW. Threshold and suprathreshold perceptual colour differences. J Opt Am 1973;63(5):615–25. https://doi.org/10.1364/JOSA.63.000615. 1973.

[44] Duce C, Della Porta CV, Tiné MR, Spepi A, Ghezzi L, Colombini ME, et al. FTIR study of ageing of fast drying oil colour (FDOC) alkyd paint replicas. Spectrochim Acta Mol Biomol Spectrosc 2014;130:214. https://doi.org/10.1016/j.saa.2014.03.123. 2014.

[45] Ploeger R, Scalarone D, Chiantore O. The characterization of commercial artists' alkyd paints. J Cult Herit 2008;9:412–9. https://doi.org/10.1016/j.culher.2008.01.007.